African Journal of Environmental Science and Technology Vol. 4(7), pp. 446-454, July 2010
Available online at http://www.academicjournals.org/AJEST
ISSN 1991-637X ©2010 Academic Journals

Full Length Research Paper

Anomaly effects of arrays for 3d geoelectrical resistivity imaging using orthogonal or parallel 2d profiles

A. P. Aizebeokhai[1]* and A. I. Olayinka[2]

[1]Department of Physics, Covenant University, Ota, Nigeria.
[2]Department of Geology, University of Ibadan, Ibadan, Nigeria.

Accepted 20 May, 2010

The effectiveness of using a net of orthogonal or parallel sets of two-dimensional (2D) profiles for three-dimensional (3D) geoelectrical resistivity imaging has been evaluated. A series of 2D apparent resistivity data were generated over two synthetic models which represent geological or environmental conditions for a typical weathered profile and waste dump site, respectively, commonly associated with geophysical applications for hydrogeological, environmental and engineering investigations. Several minimum electrode separations and inter-line spacing were used to generate the apparent resistivity data for each electrode array with a view to determining the optimum inter-line spacing relative to the minimum electrode separation. The 2D apparent resistivity data for each array were collated to 3D data sets. The effectiveness and efficiency of the arrays in 3D geoelectrical resistivity imaging were evaluated by determining the mean absolute anomaly effects of the electrodes arrays on the synthetic models. The anomaly effects observed in dipole-dipole (DDP), pole-dipole (PDP) and Wenner-Schlumberger (WSC) arrays were generally larger than that observed in other arrays considered. The least anomaly effect on the synthetic models was observed in pole-pole (PP) array. This indicates that DDP, PDP and WSC arrays are more sensitive to 3D features. In all the arrays, the anomaly effects observed in the data set generated using the conventional square grids were slightly larger than those from parallel or orthogonal 2D profiles. This slight increase is attributed to the increased data density and is insignificant when compared with those of parallel and orthogonal 2D profiles. Hence, the use of parallel or orthogonal 2D profiles for 3D geoelectrical resistivity survey is effective.

Key words: Anomaly effects, orthogonal/parallel 2D profiles, 3D surveys, geoelectrical resistivity imaging, measurement effectiveness.

INTRODUCTION

Geoelectrical resistivity imaging has played an important role in addressing a wide variety of hydrological, environmental and geotechnical issues. The vertical electrical sounding (VES) that has been commonly adopted assumes a smooth vertical variation of the potential field with depth while lateral variations of the subsurface resistivity are thought to be constant. This assumption makes the VES technique grossly inadequate in most environmental and engineering investigations where the geology is usually complex, subtle and multi-scale such that both lateral and vertical variations of the subsurface petrophysical properties can be very rapid and erratic.

*Corresponding author. E-mail: philps_a_aizebeokhi@yahoo.co.uk. Tel: +234-803-7341-499.

Two-dimensional (2D) geoelectrical resistivity imaging, in which the subsurface resistivity is assumed to vary both laterally and vertically along the survey line but constant in the perpendicular direction, has been widely used to map areas with moderately complex geology (e.g. Griffiths and Barker, 1993; Griffiths et al., 1990; Dahlin and Loke, 1998; Olayinka, 1999; Olayinka and Yaramanci, 1999; Amidu and Olayinka, 2006). However, 2D resistivity imaging often produce misleading subsurface images due to out-of-plane resistivity anomaly, and the inherent three-dimensional nature of geological structures and subsurface petrophysical properties. Hence, a three-dimensional (3D) geoelectrical resistivity imaging should, in theory, give a more accurate and reliable picture of the subsurface, especially in highly heterogeneous subsurface commonly associated with environmental and engineering investigation sites.

What constitute a 3D data set that would yield significant 3D subsurface information for geoelectrical resistivity imaging is less understood. Ideally, a 3D geoelectrical resistivity data set should constitute a survey in which apparent resistivity measurements are made in all possible directions. In the 3D geoelectrical resistivity surveying currently in practice, electrodes are commonly arranged in square or rectangular grids with constant electrode spacing in both x- and y-directions. Most practical/large scale 3D geoelectrical resistivity surveys would involve grids in which the number of electrodes required is far more than that available in most multi-electrode resistivity systems. The roll-along technique (Dahlin and Bernstone, 1997) could be used to get around this limitation. But this technique could be tedious and cumbersome, and therefore may not be economical in large scale 3D geoelectrical resistivity imaging. Pole-pole (PP) array has been commonly used in 3D geo-electrical resistivity surveys because it has the highest number of possible independent measurements and the widest horizontal coverage.

The pole-pole array consists of one current and one potential electrode with the second current and potential electrodes at infinite distances. Finding suitable locations for these electrodes at infinity to satisfy the theoretical requirement is often difficult in practical surveys. In addition, the contributions of the electrodes at infinity to the observed data can be significant making it difficult for the measured data to satisfy the condition of reciprocity (Park and Van, 1991). Apart from these limitations, pole-pole array is highly susceptible to telluric noise capable of degrading the quality of the observed data and hence the resulting inversion models. Hence, a more realistic, practical and economical 3D data acquisition geometry for geo-electrical resistivity imaging that would allow reasonable flexibility in the choice of electrode configuration is needed.

The effectiveness and imaging capabilities of geoelectrical resistivity measurements for a given configuration of electrodes can be evaluated using the anomaly effect (Militzer et al., 1979, Dahlin and Zhou, 2004). For an effective geoelectrical resistivity survey, the value of the anomaly effect should be significantly greater than the background noise of the electrode configuration. Thus, anomaly effect is a measure of the signal-to-noise ratio of the electrode arrays and should varies with different geological models for a given electrode configuration. Geoelectrical resistivity data with high anomaly information usually produce good quality, high resolution and reliable inversion images. Field measurements are often contaminated by different kinds of noise; the noise characteristics being different for different investigation sites but usually with a general trend, and depend on the electrode array used for the measurements. Thus, the contamination of field observations with noise generally depends on the potential values measured by a particular array, and hence the observed apparent resistivity data. The anomaly effects of electrode arrays can therefore be estimated using the apparent resistivity data. The apparent resistivity data allows us to qualitatively describe the totality of the subsurface geological and petrophysical features with respect to the geometrical configurations of the electrodes used in obtaining the apparent resistivity data. Thus, the effectiveness and imaging capabilities of different electrode configurations can be suitably compared by using apparent resistivity data (and hence anomaly effect) obtained for the different electrode configurations. In this paper, a net of orthogonal or parallel sets of synthetic 2D apparent resistivity data were collated to 3D data sets which were processed using a full 3D inversion code. The relative effectiveness and imaging capabilities of selected arrays: Wenner-alpha (WA), Wenner-beta (WB), Wenner-Schlumberger (WSC), dipole-dipole (DDP), pole-dipole (PDP), and pole-pole (PP), were evaluated by determining the anomaly effects of these arrays on two synthetic models that simulates different geological conditions commonly associated with geophysical applications for hydrogeological, environmental and engineering investigations. The response of these model structures to 3D geoelectrical resistivity surveying with a combination of orthogonal or parallel sets of 2D profiles for different electrode configurations was assessed using anomaly effects of the arrays which is a measure of the signal-to-noise ratio. The optimum spacing between the orthogonal or parallel sets of 2D profiles (inter-line spacing) relative to the minimum electrode separation required to form a significant 3D data set that would yield reasonable 3D inversion model was also evaluated.

SYNTHETIC MODELS DESCRIPTION

In order to investigate the capabilities of different electrode configurations in 3D geoelectrical resistivity imaging using a combination of orthogonal or parallel sets of 2D profiles, two synthetic model geometries representing different geological or environmental conditions were designed.

The first is a horst model structure that simulates a typical weathered or fractured profile in a crystalline basement complex in tropical areas, while the other is a trough model structure used to simulate the geological conditions of a typical waste dump site which is usually complex and subtle. These two geological conditions are commonly associated with geophysi-cal applications for hydrogeological, environmental and engineering investigations. Hence, it is important to investigate the response of these structures to 3D geoelectrical resistivity surveying with a combination of orthogonal or parallel sets of 2D resistivity imaging for different electrode configurations.

A three-dimensional (3D) horst structure under an area of 100 x 100 square meters (Figure 1), with lateral variation in the thickness such that the horst thickens towards the centre of the model where the least weathering is thought to occur and thinning outward with increasing weathering activities, was assumed. The horst structure consists of a three layers model comprising of the top soil, saprolite (the weathered zone) and the fresh basement. The top layer, corresponding to the top soil, was assigned a uniform thickness of 2.5 m and its resistivity varies laterally between $500\Omega m$, $700\Omega m$ and $400\Omega m$ from left to right. The weathered zone, represented with the thickness of the middle layer in the model structure, is

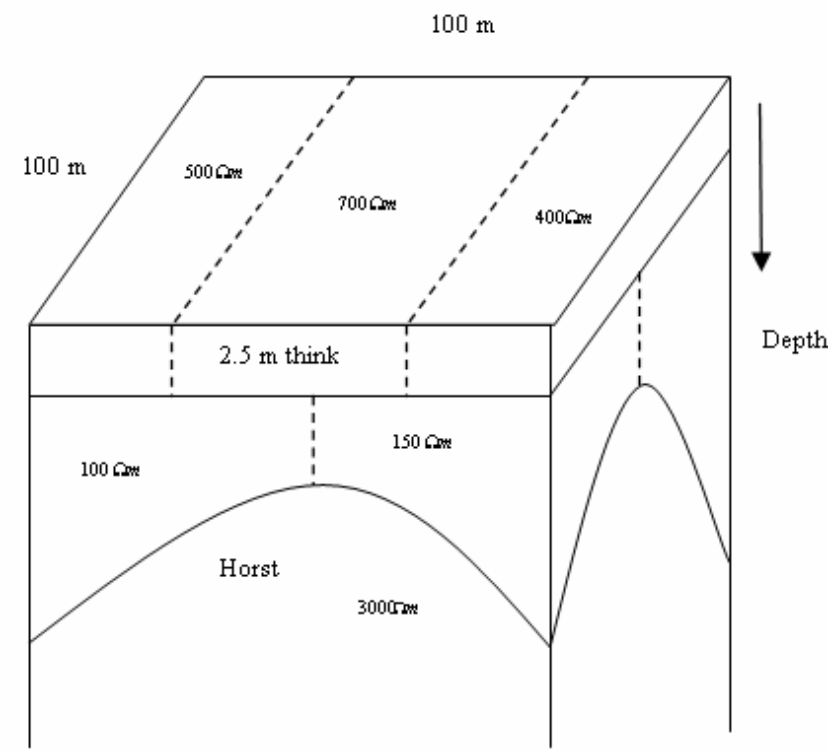

Figure 1. A three-dimensional horst model simulating a typical weathered or fractured profile developed above crystalline basement complex.

thought to have undergone various lateral degrees of weathering or fracturing that increases outward. The thickness of the weathered zone was assumed to vary between a minimum of 5.75 m (depth 8.25 m) at the centre of the model structure where the least weathering occurs to a maximum of 13.50 m (depth 16.0 m) at the edges of the model considered to be most weathered. The weathered zone in crystalline basement complex is a product of chemical weathering which is usually a low resistive saprolite overlying a more resistive basement rocks (Carruthers and Smith, 1992; Hazell et al., 1992). In addition, this zone is commonly aquiferous, thus low resistivity model values varying between $100\Omega m$ and $150\Omega m$ was assigned to this layer. Underlying the weathered zone is a fresh basement of infinite thickness with a constant model resistivity value of $3000\Omega m$.

Similarly, the second synthetic model is a three-dimensional (3D) trough structure also thought to be under an area of 100 x 100 square meters (Figure 2), for convenience of electrode layouts. The synthetic trough model consist of three layers in which the thicknesses of the top and the middle layers varies with a maximum of 4.2 and 11.8 m, respectively, and the underlying third layer is a basement rock of infinite thickness. The trough structure is assumed to be at the centre of the model with varying lateral thickness and cutting across the first and second layers. Model resistivities values of $300\Omega m$ and $600\Omega m$ are assigned to the first and second layers, respectively, in their natural states. The trough structure and its surroundings are thought to be impacted by the deposited waste in the simulated dump site and hence would consist of laterally varying low resistivity values. Model resistivity values varying laterally between $50\Omega m$ and $250\Omega m$, different from the assigned value of $300\Omega m$ in its natural state, were therefore assigned to the trough structure. Part of the second layer underlying the trough structure is also thought to be impacted by leachates from the deposited waste so that its model resistivity value varies to a minimum of $400\Omega m$ from the assigned value of $600\Omega m$ in its natural state. The leachates from the deposited waste in the simulated dump site is thought not to have reach the basement, thus its resistivity would be approximately constant laterally. A constant model resistivity value of $2500\Omega m$ was therefore assigned to the underlying basement of infinite thickness.

DETERMINATION OF APPARENT RESISTIVITY AND ANOMALY EFFECTS

The 3D synthetic model structures were approximated into series of 2D model structures separated with a constant interval in both parallel and perpendicular directions. Synthetic apparent resistivity data were calculated over the resulting orthogonal sets of 2D profiles using RES2DMOD forward modeling code for the selected arrays. The parallel 2D profiles which run in the west-east direction were denoted as in-lines while those in the perpendicular direction were denoted as cross-lines. Electrode layouts with different minimum separations, *a* and inter-line spacing, *L* (*a* = 2, 4, 5 and 10 m; *L* = *a*, 2*a*, 2.5*a*, 4*a*, 5*a* and 10*a)* were used in the calculation of the apparent resistivity data. The series of 2D model structures were subdivided into a number of homogeneous and isotropic blocks using a rectangular mesh. The model resistivity value of each block in the mesh was supplied using an input text file. The 2D modeling accounts for 3D effect of current sources; thus the resistivity of each of the model was allowed to vary arbitrarily along the profile and with depth, but with an infinite perpendicular extension.

The finite difference method (Dey and Morrison, 1979), which

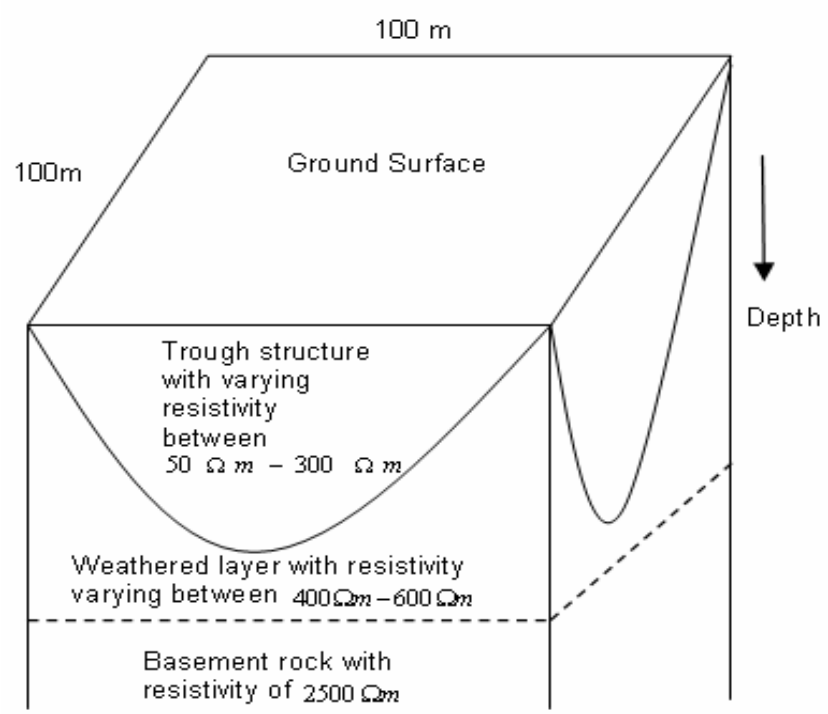

Figure 2. A three-dimensional trougmodel simulating the geology of a waste dump site.

basically determines the potentials at the nodes of the rectangular mesh, was employed in the calculation of the potential distribution. A double precision, which slightly takes a longer time but significantly more accurate, was used in the calculations of the potential distribution. The apparent resistivity values were normalized with the values of a homogeneous earth model so as to reduce the errors in the calculated potential values. The calculation errors are often less than 5%. The forward modeling grid used consists of four nodes per unit electrode. The calculated apparent resistivity values for each 2D profile for the different geological models were contaminated with 5% Gaussian noise (Press et al., 1996) so as to simulate field conditions. The synthetic apparent resistivity data computed for the series of approximated 2D model structures were then collated to 3D data sets using RES2DINV inversion software (Loke and Barker, 1996). During the data collation, the coordinates, line direction and electrodes of each 2D profiles were supplied to the computer program via a text file. The collations arranged the 2D apparent resistivity data and the electrode layouts in rectangular or square grids pattern according the coordinates and direction of each profile used, and electrodes positions in the profile. Thus, the number of electrodes in each 2D profile, number of profiles collated and their directions determine the size and pattern of the electrode grid obtained. These parameters along with the data level attained for each array determine the data density of the resulting 3D data set. The 3D apparent resistivity values were then assessed and used to estimate the anomaly effects of the arrays on the synthetic models. The mean absolute anomaly effect on the models for a given electrode configuration was defined as:

$$AE = \frac{\rho_{\max} - \rho_{\min}}{\rho_{av}}, \qquad 1$$

Where $\rho_{\max}$, $\rho_{\min}$ and ρ_{av} are maximum, minimum and average apparent resistivities, respectively, observed for the electrode configuration.

RESULTS AND DISCUSSION

The mean absolute anomaly effects of the selected arrays on the synthetic models – horst and trough models – using 3D data sets collated from orthogonal 2D profiles are given in Figures 3 and 4, respectively. The mean anomaly effects for the various electrode grid sizes and inter-line spacing relative to the minimum electrode separation are presented. Similarly, the anomaly effects produced on the synthetic models by collating only parallel set of 2D apparent resistivity data to obtain 3D data set are given in Figures 5 and 6, respectively. Similar trends in the anomaly effects are observed for both the 3D data sets collated from in-line profiles (2D profiles in the west - east direction) and cross-line profiles(2D profiles in the north - south direction), and are comparable to those observed in the 3D data sets collated from the orthogonal 2D profiles. The observed anomaly effects of the orthogonal profiles on the synthetic models are however higher than those observed for parallel profiles. This indicates that the 3D model images that would be produced by inverting the data set collated from orthogonal profiles are superior to those produced by inverting the data set collated from parallel profiles. In general, electrode arrays with high anomaly effects on geological models or subsurface structures will usually

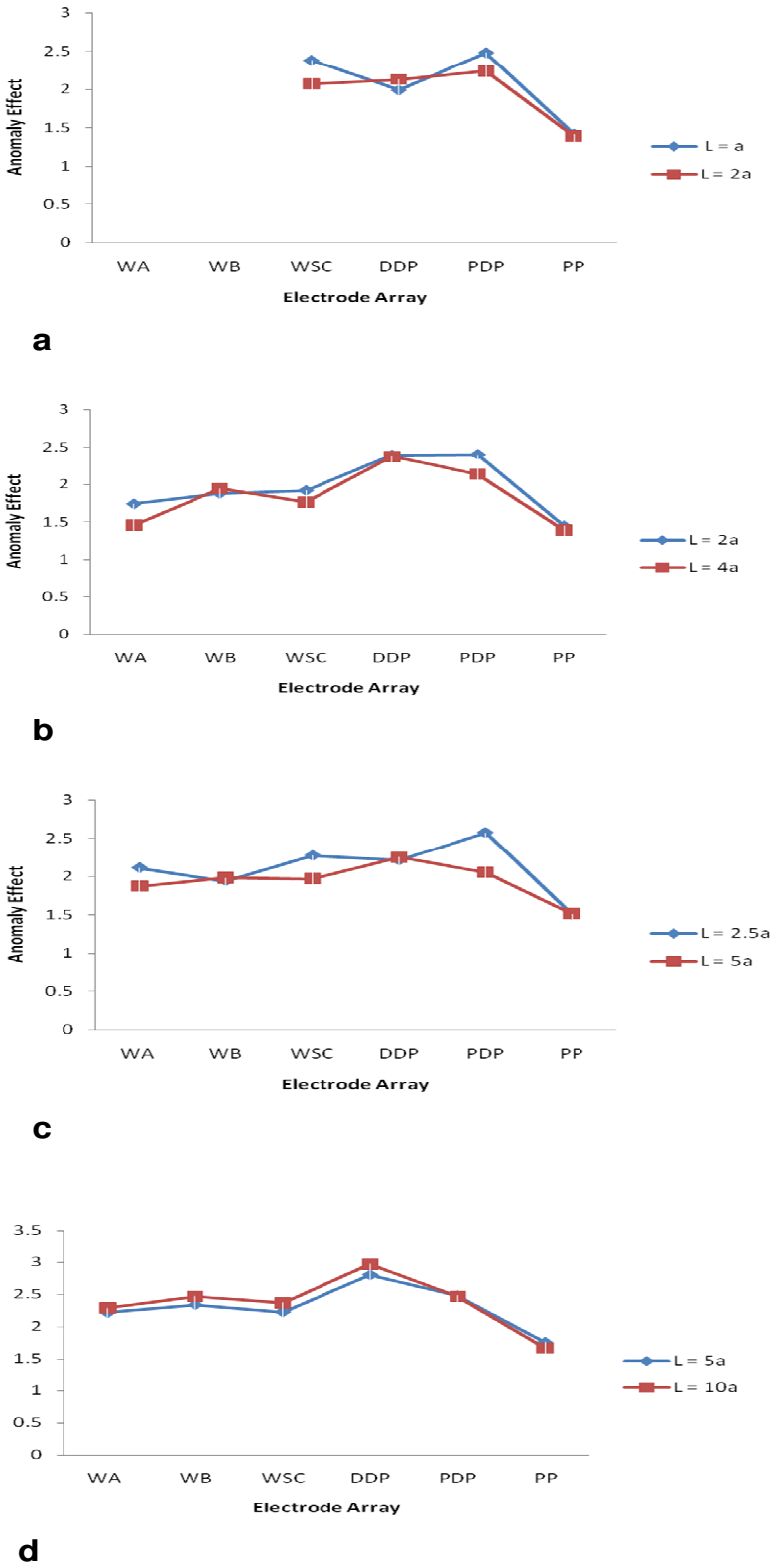

Figure 3. Mean absolute anomaly effect of electrode arrays on the horst synthetic model; 3D geoelectrical resistivity imaging using orthogonal set of 2D profiles with grid size: (a) 11x11 (b) 21 x 21, (c) 26 x 26 ($L=5a$) and 31 x 31 ($L=2.5a$), and (d) 51 x 51; L is inter-line spacing and a is the minimum electrode separation.

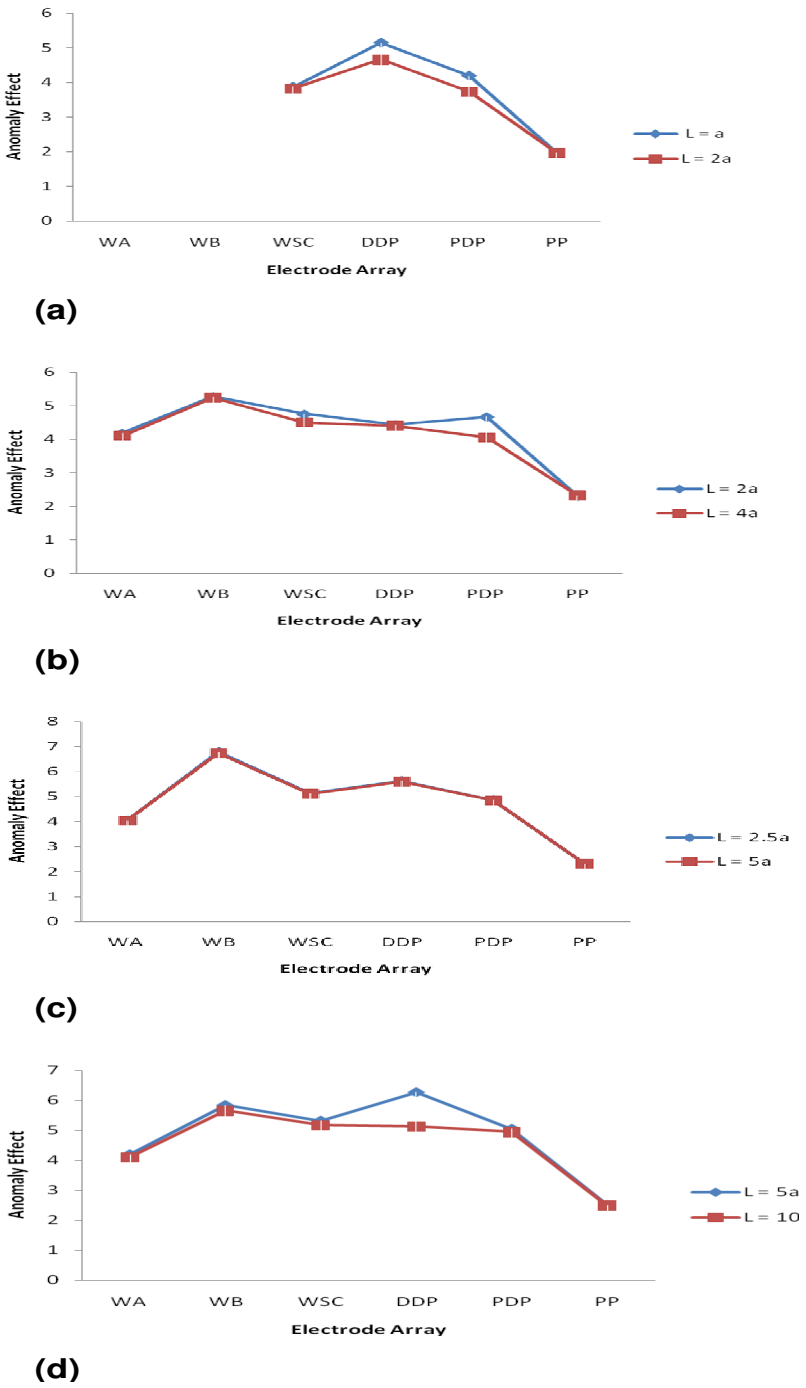

Figure 4. Mean absolute anomaly effect of electrode arrays on the trough synthetic model; 3D geoelectrical resistivity imaging using orthogonal set of 2D profiles with grid size: (a) 11x11 (b) 21 x 21, (c) 26 x 26 ($L=5a$) and 31 x 31 ($L=2.5a$), and (d) 51 x 51; L is inter-line spacing and a is the minimum electrode separation.

produce better signal-to-noise ratio than electrode arrays with low anomaly effects on the same geological models or subsurface structure (Dahlin and Zhou, 2004). Consequently, arrays with high anomaly effects will yield inversion images with better resolution and model sensitivity than arrays with low anomaly effects. The anomaly effect of any electrode configuration varies from geological model to geological model depending on the

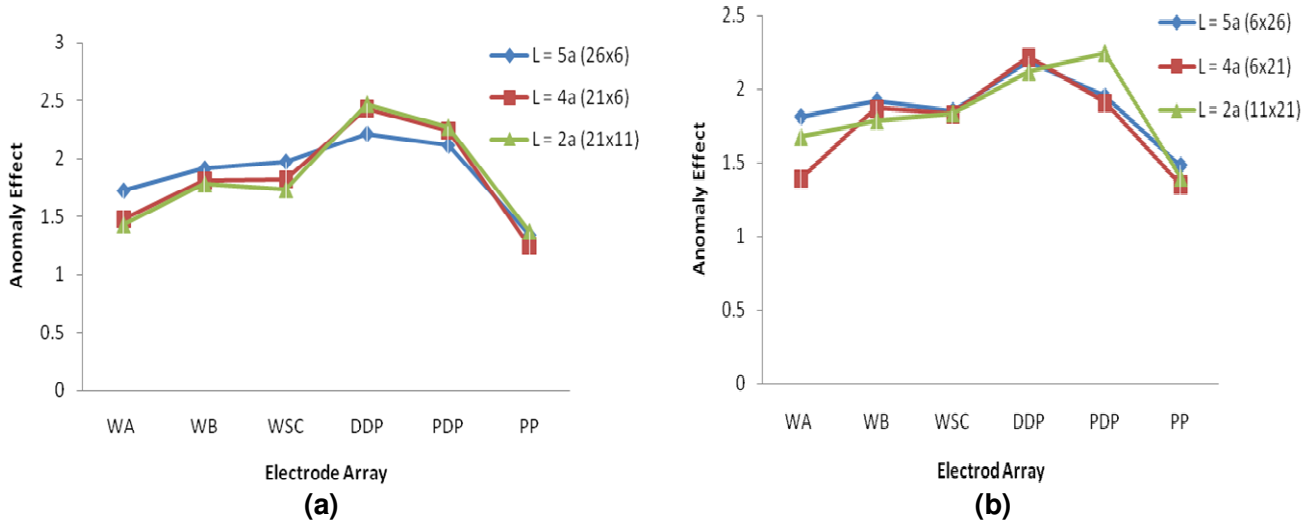

Figure 5. Mean absolute anomaly effect of electrode arrays on the horst synthetic model; 3D geoelectrical resistivity imaging using parallel set of 2D profiles: (a) In-line profiles, and (b) cross-line profiles.

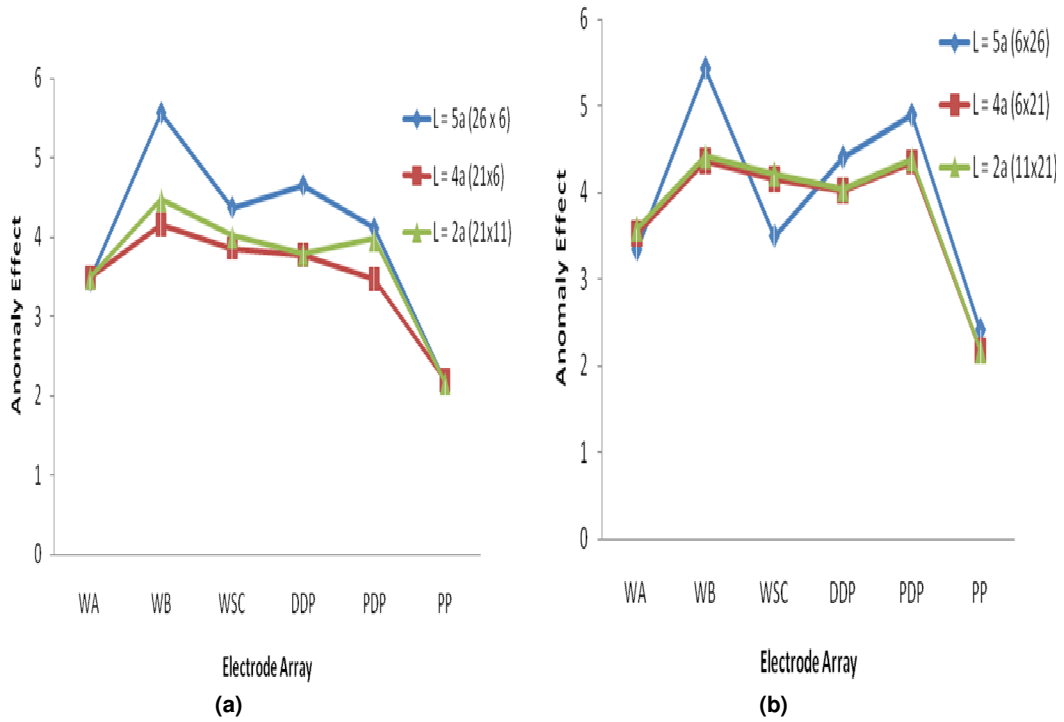

Figure 6. Mean absolute anomaly effect of electrode arrays on the trough synthetic model; 3D geoelectrical resistivity imaging using parallel set of 2D profiles: (a) In-line profiles, and (b) cross-line profiles.

resistivity contrast and the general background noise level (Dahlin and Zhou, 2004). In Figures 3 to 6, the anomaly effects of the arrays on the trough model is generally higher than those observed on the horst model. The dipole-dipole (DDP), pole-dipole (PDP) and Wenner-Schlumberger (WSC) arrays produced larger anomaly effects on the horst model than the other arrays investigated. Similarly, Wenner-beta (WB), dipole-dipole (DDP) and pole-dipole (PDP) arrays generally yield much larger anomaly effects on the trough model than any of the other arrays. In both synthetic models, the pole-pole (PP) array gives the smallest anomaly effect. The anomaly

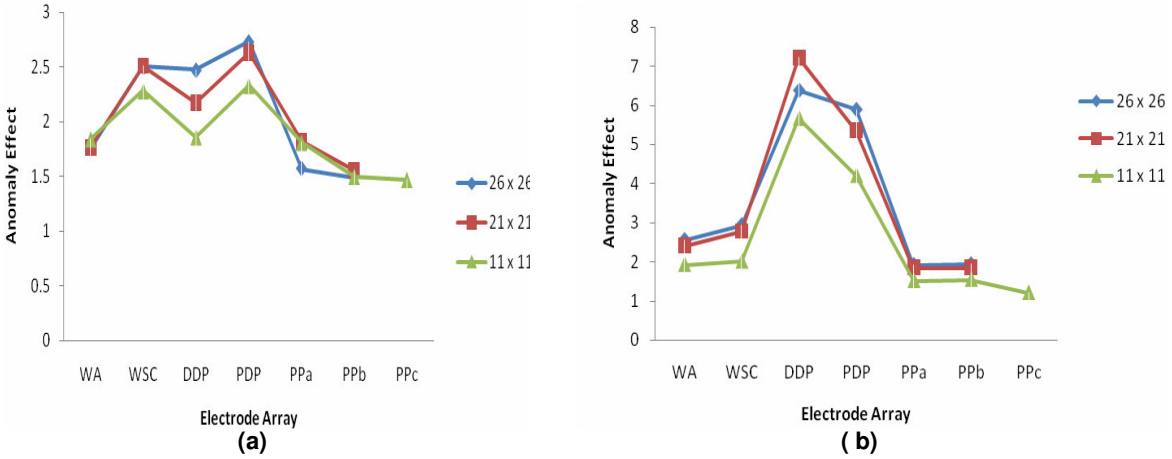

Figure 7. Mean absolute anomaly effects of electrode arrays on: (a) horst and (b) trough models; conventional 3D resistivity imaging using square or rectangular grids of electrodes.

effect of the arrays on the synthetic models is largely dependent on the electrode grid size (or minimum electrode separation) and data density. The anomaly effect on the synthetic models generally increases with increasing data density which depends on the minimum electrode separation, a and data level, n used in the computation of the apparent resistivity data as well as the electrode grid size and inter-line spacing L between the 2D lines. The anomaly effects shown in Figures 3 to 6 are compared with the electrode grid size and inter-line spacing L relative to the minimum electrode separation. The dependence of the anomaly effect of array on the inter-line spacing relative to the minimum electrode separation used in the determination of the apparent resistivity values could not be established. However, the results show that the anomaly effect increases with decreasing inter-line spacing. We suggests that inter-line spacing equal or less than $4a$, where a is the minimum electrode separation would yield high resolution inversion images.

Conclusion

These results generally suggest that the resolution and sensitivity of the 3D model inversion images for data sets that would be obtained using DDP, PDP and WSC arrays for the orthogonal or parallel 2D profiles would be better than those of other arrays. Pole-pole array would yield the least model resolution and sensitivity; and this could be due to the fact that pole-pole array is more prone to picking telluric noise that any other array. Anomaly effects of electrode arrays on the synthetic models for conventional 3D surveys in which 3D apparent resistivity measurements are made with square or rectangular grids of electrodes were also determined and are given in Figure 7. In all the arrays, the anomaly effects observed in the data set generated using the conventional square or rectangular grids of electrodes were slightly larger than those from parallel or orthogonal 2D profiles. This slight increase in anomaly effects is attributed to the increased data density. Thus, the observed slight increased in the between the anomaly effects on the synthetic models presented in Figure 7 cannot be said to be significant. This shows that, on the basis of the analysis of anomaly effects of electrode configuration on the geological models, collating parallel or orthogonal sets of 2D apparent resistivity data to 3D data set is an effective and efficient technique in 3D geoelectrical resistivity imaging surveys. Since the optimum inter-line spacing relative to the minimum electrode separation between the orthogonal or parallel 2D profiles could not be ascertained, other techniques should be device to determine the optimum inter-line spacing relative to the minimum electrode separation that would yield good quality, high resolution and reasonable 3D model inversion images.

REFERENCES

Amidu SA, Olayinka AI (2006). Environmental assessment of sewage disposal systems using 2D electrical resistivity imaging and geochemical analysis: A case study from Ibadan, Southwestern Nigeria. Environ. Eng. Geosci., 7(3): 261-272.

Carruthers RM, Smith IF (1992). The use of ground electrical survey methods for sitting water supply boreholes in shallow crystalline basement terrain. In: Wright, E. P. and Burgess, W. G. (Eds.), Hydrogeology of Crystalline basement Aquifers in Africa. Geol. Soc. Special Public., 66: 203-220.

Dahlin T, Bernstone C (1997). A roll-along technique for 3D resistivity data acquisition with multi-electrode arrays. Proceedings SAGEEP'97, Reno, Nevada. pp. 927-935.

Dahlin T, Loke MH (1998). Resolution of 2D Wenner resistivity imaging as assessed by numerical modelling. J. Appl. Geophy., 38(4): 237-248.

Dahlin T, Zhou B (2004). A numerical comparison of 2D resistivity imaging with 10 electrodes array. Geophysical Prospecting, 52: 379-398.

Dey A, Morrison HF (1979). Resistivity modelling for arbitrary shaped two-dimensional structures. Geophy. Prospecting, 27: 1020-1036.

Griffiths DH, Barker RD (1993). Two dimensional resistivity imaging and modelling in areas of complex geology. J. Appl. Geol. 29: 211-226.

Griffiths DH, Turnbull J, Olayinka AI (1990). Two-dimensional resistivity mapping with a complex controlled array. First Break, 8(4): 121-29.
Hazell JRT, Cratchley CR, Jones CRC (1992). The hydrology of crystalline aquifers in northern Nigeria and geophysical techniques used in their exploration. In: Wright, E. P. and Burgess, W. G. (Eds.), Hydrogeology of Crystalline basement Aquifers in Africa. Geol. Society Special Publication, 66: 155-182.
Loke MH, Barker RD (1996). Practical techniques for 3D resistivity surveys and data inversion. Geophysical Prospecting, 44, p. 499-524.
Militzer H, Rosler R, Losch W (1979). Theoretical and experimental investigations of cavity research with geoelectrical resistivity methods. Geophysical Prospecting, 27: 640-652.
Olayinka AI (1999) Advantage of two-dimensional geoelectrical imaging for groundwater prospecting: case study from Ira, southwestern Nigeria. J. Nat. Ass. Hydrogeol., 10: 55-61.
Olayinka AI, Yaramanci U (1999). Choice of the best model in 2-D geoelectrical imaging: case study from a waste dump site. European J. Environ. Eng. Geophys., 3: 221-244.
Park SK, Van GP (1991). Inversion of pole-pole data for 3D resistivity structure beneath arrays of electrodes. Geophysics, 56: 951-960.
Press WH, Teukolsky SA, Vetterling WT, Flannery BP (1996). Numerical recipes in Fortran 77: The Art of Scientific Computing, 2nd edn., Cambridge University Press.